

# **DEVELOPING FLOW IN MICROCHANNEL HAVING REGULAR MICROSTRUCTURE**

By:

**TAN YAN XU**

(Matrix No : 125049)

Supervisor:

**Dr Yu Kok Hwa**

May 2018

This dissertation is submitted to

Universiti Sains Malaysia

As partial fulfillment of the requirement to graduate with honors degree in

**BACHELOR OF ENGINEERING (MECHANICAL ENGINEERING)**



**UNIVERSITI SAINS MALAYSIA**

School of Mechanical Engineering

Engineering Campus

Universiti Sains Malaysia

## **DECLARATION**

It is declared that the content of the dissertation titled Developing Flow in Microchannel Having Regular Microstructure has been prepared in part me, Tan Yan Xu Wherever contributions of others are involved, every effort is made to indicate this clearly, with due reference to the literature, and acknowledgement of collaborative research and discussions. It is further declared that this is my original work, as part of the requirement for a course titled EMD 452 Final Year Project for a Mechanical Engineering degree at the School of Mechanical Engineering, Universiti Sains Malaysia. The work was done under the guidance of Dr Yu Kok Hwa who is a lecturer of School of Mechanical Engineering, Universiti Sains Malaysia.

---

Signature

Name: Tan Yan Xu

Date:

In my capacity as supervisor of the candidate's thesis, I certify that the above statements are true to the best of my knowledge.

---

Signature

Name: Dr Yu Kok Hwa

Date:

## **ACKNOWLEDGEMENT**

Without the support of the following people, the work presented in this dissertation would not have been possible. For this reason, I would like to extend my sincere appreciation to my final year project, Dr Yu Kok Hwa whose contribution in stimulating suggestions and encouragement, helped me to coordinate my project especially in writing this report and also guiding me in the ANSYS FLUENT Simulation and data extraction and processing.

Furthermore I would also like to acknowledge with much appreciation the crucial role of the staff of Computer Aided Design (CAD) Lab of School of Mechanical Engineering, Mr Jamari Bin Sadli, who gave the permission to use the computer in CAD Lab for running simulation on developing flow in microchannel having regular microstructure as well as his willingness to come to Mechanical School on holiday to open the CAD Lab for me to reset my disconnected Teamviewer connection towards computer in CAD Lab. I have to appreciate the guidance given by other supervisor as well as the panels especially in my project presentation that has improved my presentation skills thanks to their comment and advices.

Besides that, I also want to appreciate my friends who teach and guide me patiently on ANSYS FLUENT as I am a newbie on this software. Last but not least, I want to thank to my family for their unconditional love, spiritual and moral support which is always available and lasts for eternity.

## TABLE OF CONTENTS

i) List of Figure .....	i
ii) List of Tables .....	iii
iii) List of Abbreviation.....	iv
iv) Abstrak.....	v
v) Abstract .....	vi
<b>CHAPTER 1: INTRODUCTION.....</b>	<b>1</b>
1.1 Brief Overview .....	1
1.2 Objective .....	3
1.3 Problem Statement.....	3
1.4 Scope of Work.....	7
<b>CHAPTER 2: LITERATURE REVIEW .....</b>	<b>8</b>
2.1 Research Background.....	8
<b>CHAPTER 3: RESEARCH METHODOLOGY .....</b>	<b>10</b>
3.1 Constraint and Flow Condition in Microchannel .....	10
3.2 Creation of Microchannel Model .....	11
3.3 Ansys Simulation .....	16
3.4 Data Acquisition and Analysis .....	22
<b>CHAPTER 4: RESULT AND DISCUSSION.....</b>	<b>23</b>
4.1 Results of Grid Independence Test .....	23
4.2 Results of Validation on Previous Studies .....	29
4.3 Results of Simulation of Parallel Plate Microchannel .....	31
4.4 Results of Simulation of Rectangular Microchannel .....	37
4.5 Discussion .....	43
<b>CHAPTER 5: CONCLUSION AND FUTURE WORK .....</b>	<b>47</b>
<b>REFERENCE .....</b>	<b>49</b>
<b>APPENDICES .....</b>	<b>52</b>

## LIST OF FIGURES

Figure	Title	Page
1.1	Development of fluid flow in the entrance region.	2
3.1	Flow Chart of Research Methodology	10
3.2	Schematic Diagram for Type of Regular Microstructure in Rectangular Microchannel and Parallel Plate Microchannel	11
3.3	Schematic Diagram for Parameter and Sizing of Microstructure	12
3.4	Parameter of microstructure for both transverse (i) and longitudinal (ii) groove, (iii) Shear free region of 2D model parallel plate microchannel with transverse groove. (iv) Shear free region of 3D model rectangular microchannel with longitudinal groove	13
3.5	(i) Split by Delta, (ii) Split by N	15
3.6	(i) Perpendicular green straight line joining the points along two parallel edges, (ii) Resultant Split surfaces	16
3.7	(i) Mesh element of 2D model, (ii, iii, iv) Relevant edges for meshing operation of 3D transverse groove model, (v, vi, vii, viii) Relevant edges for meshing operation of 3D longitudinal groove model	17-19
3.8	(i) Boundary Condition for 2D model of Parallel Plate Microchannel with Transverse Groove and Smooth Surface (ii) Boundary Condition for 3D model of Rectangular Microchannel with Transverse Groove (iii) Boundary Condition of 3D model of Rectangular and Parallel Plate Microchannel with Longitudinal Groove	20
4.1	Dimension indication for (i) 2D model and (ii) 3D model	23

4.2	Grid Independence Test for (i) Parallel Plate Microchannel with smooth surface (ii) Parallel Plate Microchannel with transverse groove of different L and percentage of no slip condition. (iii) Parallel Plate Microchannel with longitudinal groove.	24-25
4.3	Grid Independence Test for (i) Rectangular Microchannel with smooth surface (ii) Rectangular Microchannel with transverse groove (iii) Rectangular Microchannel with longitudinal groove	27-28
4.4	Validation for (i) Parallel Plate Microchannel (ii) Rectangular Microchannel	30
4.5	Velocity Profile for Parallel Plate Microchannel of Transverse Groove varies with (i) different No Slip Fraction and (ii) different value of L	32-33
4.6	Velocity Profile at (i) Shear Free surface and (ii) No Slip Surface for Parallel Plate Microchannel of Longitudinal Groove varies with different percentage of No Slip Fraction. Velocity Profile at (iii) Shear Free surface and (iv) No Slip Surface for Parallel Plate Microchannel of Longitudinal Groove varies with L	35-36
4.7	Velocity Profile for Rectangular Microchannel of Transverse Groove varies with (i) different No Slip Fraction and (ii) different value of L.	38-39
4.8	Velocity Profile at all the (i) no slip surfaces and (ii) shear free surfaces for Rectangular Microchannel of Longitudinal Groove varies with L=0.1 and 25% No Slip Fraction. Velocity Profile at (iii) no slip surfaces and (iv) shear free surface for rectangular Microchannel of Longitudinal Groove varies with L	41-42

## LIST OF TABLES

Table	Title	Page
1.1	Coefficient in Equation 1 and 2	4
4.1	Grid Independence Test for Parallel Plate Microchannel	26
4.2	Grid Independence Test for Rectangular Microchannel	28
4.3	Validation for parallel plate microchannel and rectangular microchannel	31
4.4	Results of simulation for Parallel Plate Microchannel with Transverse Groove	32
4.5	Results of simulation for Parallel Plate Microchannel with Longitudinal Groove.	34
4.6	Results of simulation for Rectangular Microchannel with Transverse Groove.	38
4.7	Results of simulation for Rectangular Microchannel with Longitudinal Groove.	40
5.1	Effect on dimensionless period extent of groove-rib combination, $L$ and no slip fraction $\delta$ on parallel plate microchannel with transverse groove and longitudinal groove	47
5.2	Effect on dimensionless period extent of groove-rib combination, $L$ and no slip fraction $\delta$ on rectangular microchannel with transverse groove and longitudinal groove	47

## **LIST OF ABBREVIATION**

### Latin Symbol

- $A_c$  Cross sectional area
- $a$  Width of rectangular microchannel
- $b$  Length of rectangular microchannel
- $D_h$  Hydraulic diameter
- $E$  Length for a period of combination of no slip wall (rib)  
with the shear free fraction (groove),
- $e$  Length for shear free fraction,
- $H$  Height of microchannel
- $L_e$  Hydrodynamic entrance length
- $P_w$  Wetted perimeter
- $H$  Height of microchannel
- $h$  Heat transfer coefficient

### Greek Symbol

- $\delta$ . No slip fraction
- $\alpha$  Aspect ratio

### Dimensionless Group

- $L$  Dimensionless period extent of groove-rib combination
- $Re$  Reynold Number



## ASBTRAK

Mikrosaluran sering digunakan dalam pakej elektronik sebagai penukar haba berpadat ataupun mikro penyejuk dalam banyak system kejuruteraan. Prestasi sistem bergantung kepada pembangunan aliran laminar dalam mikrosaluran. Kadang kala, kepanjangan mikrosaluran yang tidak mencukupi mengakibatkan aliran dalam mikrosaluran tidak dapat berkembang menjadi aliran yang berpembangunan sepenuh. Dengan kata lain, hanya aliran berpembangunan sepenuh dapat mengalir dengan lancar melalui mikrosaluran. Oleh itu, keperluan untuk menentukan jarak minimum untuk aliran dalam mikrosaluran untuk berkembang menjadi aliran berpembangunan sepenuh adalah sangat penting. Objektif utama kajian ini akan memberi perhatian dalam meneroka kesan kewujudan permukaan yang mempunyai kepelbagaian topologi ke atas kawasan kemasukan hidrodinamik mikrosaluran. Kajian ini dijalankan dengan menggunakan ANSYS FLUENT 16.1, sebuah pakej perisian yang berasaskan pengiraan jilid terhingga aliran dinamik ataupun dikenali sebagai “Computational Fluid Dynamics” (CFD) untuk mensimulasikan aliran dalam mikrosaluran yang berbentuk segi empat tepat dan berorientasi plat selari yang mempunyai mikrostruktur. Data yang didapati melalui simulasi akan diproses dengan menggunakan MATLAB untuk menentukan kepanjangan kemasukan hidrodinamik. Seperti yang dijangka, mikrostruktur mempunyai kesan atas kepanjangan kemasukan hidrodinamik sama ada dengan peningkatan ataupun pengurangan bagi mikrosaluran segi empat tepat dan plat selari mikrosaluran. Parameter mikrostruktur yang terlibat termasuk noktah tanpa dimensi yang mengandungi gabungan alur dan rusuk,  $L$  dan pecahan ketidakgelinciran  $\delta$ .

## **ABSTRACT**

Microchannel is used as compact heat exchangers or microcoolers in electronics packaging in many engineering system. The system performance depends on laminar flow development in the microchannels. Sometimes, the use of short microchannel lengths is insufficient to yield a fully developed flow. In other words, only developing flow could prevail along the channel length. Thus, it is essential to determine the distance needed for a flowing liquid before a fully developed flow condition could prevail. The main objective of the work is focused on exploring the effects of different surface topologies on the hydrodynamic entrance region in the channels. This study is carried out by using ANSYS FLUENT 16.1, a finite volume based computational fluid dynamics (CFD) software package to simulate the fluid flow in parallel plate and rectangular microchannel having regular microstructure. The data obtained from the simulation are then processed by using MATLAB to determine the hydrodynamic entrance length. As expected, regular microstructure has the effect on hydrodynamic entrance length of both increasing and decreasing the hydrodynamic entrance length of parallel plate and rectangular microchannel with its microstructure parameter of dimensionless period extent of groove-rib combination,  $L$  and no slip fraction  $\delta$ .

## **CHAPTER 1: INTRODUCTION**

### 1.1 Brief Overview

In this study, the focus is on the determination on the effect of different surface topologies on the hydrodynamic entrance region in microchannel. Hydrodynamic entrance region is referred to the distance of a flow travels after entering a pipe before the flow becomes fully developed. The length of the entry region is known as entrance length. Sometimes, the channel length for microchannel used in microdevice has short length and lead to the failure of yielding developing flow. Fully developed flow plays an important role in heat transfer and fluid flow as only developing flow can prevail along the channel and therefore carry more heat energy from the heat source. Microchannel is usually used as heat exchangers in diverse field includes aerospace, automotive, bioengineering, cooling of gas turbine blade, power and process industries and etcetera. This is because microchannel offers advantage due to their high surface to volume ratio and small volume. The large surface to volume ratio result in high rate of heat and mass transfer, making microdevice as ideal and excellent tools for compact heat exchanger.

There are many factors which affect the hydrodynamic entrance length in microchannel, i.e., microchannel inlet geometry, hydraulic diameter of the microchannel and Reynold number. Over the years, there are many research works carried out to determine the entrance length in microchannel due to the mentioned factors by finding the correlation between dimensionless entrance length and the Reynold number. Validation on previous studies has to be done first before proceeding to this study to ensure the accuracy and credibility of this study as flow in microchannel is totally different to that of macroscale flow in pipe since there is no existing correlation for reference.

Fluid flow through microchannel was first proposed by Tuckerman and Pease in 1981. In their study, they demonstrated fluid flow through microchannel as an effective means of removing heat from silicon integrated circuits. The focus of their study is on the heat removal through microchannel heat sink that is applicable to high-speed, high-density, very-large-scale integrated (VLSI) circuits as these circuits effective heat removal or cooling system due to high heat generation. They discover that the convective heat-transfer coefficient,  $h$  between the substrate and the coolant

was found to be the primary hindrance in achieving low thermal resistance. For laminar flow in confined channels,  $h$  is inversely proportional to channel width which implies microscopic channels is more desirable to be used as heat dissipation apparatus. Thus, thermal resistance can thus be further reduced by using high-aspect ratio channels to increase surface area. [1]

In macroscale fluid mechanics, when a fluid enters a circular pipe with uniform velocity, the fluid particles in the layer which is in contact with the surface of the pipe come to a complete stop since no-slip condition prevails along the wall. At the same time, this layer causes the fluid particle in the adjacent layer to decrease in speed gradually due to friction. As a compensation for velocity reduction, the velocity of the fluid at the midsection of the pipe has to be sped up so that the mass flow rate through the pipe is constant. Thus, a velocity profile is developed along the pipe. A region of the flow, known as velocity boundary layer or just the boundary layer is formed due to the effects of the viscous shearing force caused by fluid viscosity. This hypothetical boundary surface splits the flow in pipe into two different regions which are the boundary layer region, in which the viscous effects and the velocity changes are significant, and the irrotational (core) flow region, in which the frictional effects are negligible and the velocity remains virtually constant in the radial direction. The thickness of this boundary layer keep increasing in the flow direction until it reaches the pipe center and therefore fills the entire pipe, as shown in the Figure 1.1.

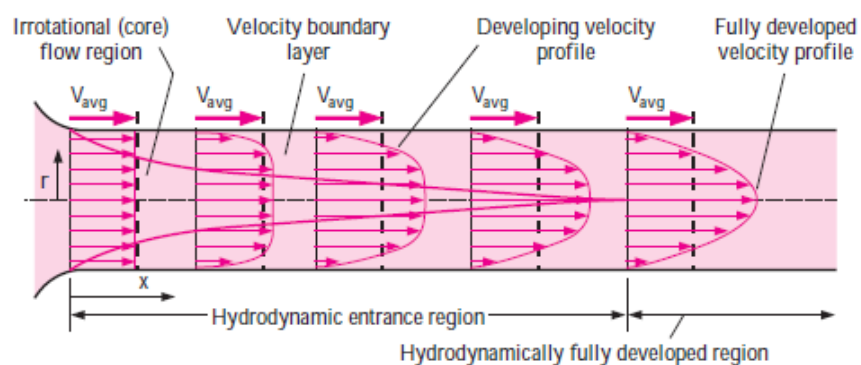


Figure 1.1: Development of fluid flow in the entrance region. [2]

The region from the pipe inlet to the point at which the merging point of boundary layer at centreline is called the hydrodynamic entrance region and the length of this region is called the hydrodynamic entrance length,  $L_e$ . Hydrodynamically developing flow is the

flow in this region where the velocity profile develops. Beyond the entrance region, the region is known as hydrodynamically fully developed and flow is called the hydrodynamically fully developed flow where the velocity profile is fully developed and remains unchanged.

In general, heat transfer is always higher in developing flows due to lower thermal resistance of the boundary layer. In the thermal entrance region, heat is being transferred from a warmer wall temperature to the lowest temperature which is the inlet fluid temperature which implies higher heat transfer coefficient. However, the heat transfer coefficient becomes constant and result in a constant sink temperature in the flow and the bulk fluid temperature rises quickly when the thermal boundary layers merge at the center.

## 1.2 Objective

The aim of this study is to determine the hydrodynamic entrance length for developing flow in microchannel having regular microstructure or different surface topologies. The entrance length for developing flow is affected by many factors such as the channel inlet geometry, i.e., the aspects ratio for rectangular microchannel, hydraulic diameter and Reynold number. For microchannel having regular structure, the effects on entrance length is expected to be substantial. Therefore, in this study, aside from considering the effect of the above factors on entrance length except hydraulic diameter and aspect ratio, the effect of regular microstructure is taken into consideration as well.

## 1.3 Problem Statement

From the previous studies carried out on the developing flow in microchannel, it is found that Reynold number, hydraulic diameter and cross section of the channel, i.e., aspect ratio for rectangular microchannel plays an important role in influencing the entrance length. Based on the study carried out by Yun et al. [3] on the effects of cross section of microchannel, it can be concluded that entrance effects can be neglected for dimensionless hydrodynamic entrance lengths ( $L_e/D_h$ ) greater than 70. The study was carried out by using numerical simulations to investigate fluid flow and heat transfer in smooth rectangular microchannels. Another study on the effect of Reynolds numbers

on the entrance length which was carried out by Atkinson et al. [4] and Chen [5] shows the correlation between dimensionless entrance length,  $(L_e/D_h)$  and the Reynold number which is based on the hydraulic diameter. The study was first experimentally for macroscale flows in circular pipes and between parallel plates. The equations of correlation with respect to the above two researchers are as shown below and the coefficients  $C_1, C_2, C_3$  are listed in Table 1.1.

$$\frac{L_e}{d_h} = C_1 + C_2 Re \quad (1)$$

$$\frac{L_e}{d_h} = \frac{C_1}{C_2 Re + 1} + C_3 Re \quad (2)$$

Equation (1) was obtained through a linear combination of the creeping flow and boundary-layer type solutions. Chen [5] proposed Eq. (2) based on the solutions of Atkinson et al. [4] and Flowsand Friedmann et al. [6].

Table 1.1: Coefficient in Equation 1 and 2

Correlation	$C_1$	$C_2$	$C_3$
Atkinson et al			
Tube	0.590	0.056	-
Parallel Plate	0.625	0.044	-
Chen			
Tube	0.600	0.035	0.056
Parallel Plate	0.630	0.035	0.004

For rectangular microchannel, the study on the effect of aspect ratio and hydraulic diameter on the hydrodynamic entrance length is investigated by Galvis et al, S. Yarusevych and J. R. Culham. [7] The study is carried out via numerical simulations to evaluate the effect of Reynold number ( $50 < Re < 200$ ), hydraulic diameter ( $0.1 \text{ mm} < D_h < 0.5 \text{ mm}$ ) and channel aspect ratio ( $1 < \alpha < 5$ ) on the entrance length in rectangular microchannels. They discover that the channel aspect ratio has negligible effect on the dimensionless entrance length for  $Re > 50$ . New correlations are proposed to predict the entrance length for rectangular microchannels with  $1 < \alpha < 5$  and for  $Re < 50$ . The correlations below are the dimensionless hydrodynamic entrance length for different aspect ratio of rectangular microchannel.

$$\frac{L_e}{D_h} = \frac{0.74}{0.09Re + 1} + 0.0889Re, \quad \alpha = 1.0$$

$$\frac{L_e}{D_h} = \frac{0.715}{0.115Re + 1} + 0.0825Re, \quad \alpha = 1.25$$

$$\frac{L_e}{D_h} = \frac{1}{0.098Re + 1} + 0.9890Re, \quad \alpha = 2.5$$

$$\frac{L_e}{D_h} = \frac{1.1471}{0.034Re + 1} + 0.0818Re, \quad \alpha = 5.0$$

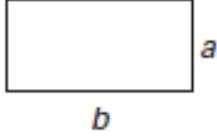
When comparing to extensive literature available on developing flows in conventional macroscale channels, limited results are available for microchannels. This is because conventional entrance length correlations comply only for a limited subset of Reynolds numbers investigated. For example, in the study of slip flow and continuum flow in circular and noncircular microchannels carried out by Duan and Muzychka in which their result accuracy is only 10% for most common duct shape. Their study involve the development of a model for predicting the Poiseuille number and the entrance length in developing slip flows and continuum flows. For the study of Renksizbulut and Niazmand [8] which involve the laminar flow and heat transfer in the entrance region of trapezoidal and rectangular channels. The correlation for the entrance length was estimated to be about 15% accurate for  $10 < Re < 1000$ . The investigated aspect ratio of rectangular channel for the study is only limited to a range of  $0.5 \leq \alpha \leq 2$ .

In this study, there is a new variable introduced that is the presence of regular microstructure at the inlet of the microchannel. It is required to determine whether the presence of regular microstructure does impose an impact on the entrance length. It is expected the presence of regular microstructure increases the hydrodynamic entrance length as it increases pressure drop along the microchannel.

The challenges in this study is the determination of the effect of regular microstructure on entrance length in conjunction with the effect of microchannel geometry as well as hydraulic geometric as well as the definition of range of Reynold Number for laminar flow in microchannel. From the perspective of channel geometry particularly for rectangular microchannel, the dimension of width and height of the

microchannel will result in the simultaneous variation of hydraulic diameter and aspect ratio. The equations for aspect ratio,  $\alpha$  and hydraulic diameter,  $D_h$  are as shown below:

For rectangular microchannel



$$\text{Aspect ratio, } \alpha = \frac{b}{a} \quad (3)$$

Hydraulic diameter is defined as the ratio of flow channel cross sectional area to the wetted perimeter.

$$D_h = \frac{4A_c}{P_w} \quad (4)$$

For rectangular microchannel,

$$D_h = \frac{4ab}{2(a+b)} = \frac{2ab}{a+b} \quad (5)$$

Therefore, it is difficult to identify the relative importance of the aspect ratio and the hydraulic diameter. In majority of the study, the effect of channel geometry was investigated by varying the channel height for a fixed channel width or vice versa by previous researchers. This method results in simultaneous change in both of the hydraulic diameter and aspect ratio which is the problem arise as mentioned before.

In terms of range of Reynold Number for laminar flow in microchannel, there is discrepancy between the studies carried out over the years. For instance, based on the study of Pfund et al. [9] the onset of laminar-to-turbulent flow transition was found to occur at a Re range of 1500–2200, where the lower value corresponds to the smaller channel depth. The range of aspect ratio and hydraulic diameter for this experiment are 0.0128–0.105 and 0.025–0.19 mm respectively. While from the study of Peng and Peterson [10], the start of the laminar-to-turbulent flow transition occurs at Re = 300, while a fully developed turbulent flow regime was first obtained at Re = 1000. The range of aspect ratio and hydraulic diameter for this experiment are 0.875–3.5 and 0.155–0.747 mm respectively. Generally, the Reynold number for laminar flow in macroscale and based on theory is 2000 and transition to turbulent flow normally occur when Reynold number is beyond this value. Based on the study carried out by Sharp K,



Adrian R and Santiago J, Molho J [11], they claim that transition to turbulence in microchannels does follow theory and that reported differences are likely due to experimental error. Therefore, from these three studies, it is difficult to determine the range of laminar flow in microchannel for a fixed velocity and hydraulic diameter which result in the difficulty to determine the hydrodynamic entrance length,  $L_e$ .

This importance of this study is to determine the minimum hydrodynamic entrance length for a flowing fluid to develop into developing flow or fully developed flow as only these two types of flow can prevail along the channel length since there is the usage of short channel lengths in many microfluidics application which is insufficient to yield a fully developed flow.

#### 1.4 Scope of Work

The scope of this study is focused on the fluid flow in microchannel, and attention is placed on determining the hydrodynamic entrance length of developing flow in microscale. The characteristics of the fluid involved in this study is single phase, incompressible, constant viscosity (Newtonian fluid) liquid while the flow is laminar flow due to small size of microchannel. For fluid-wall interaction, no slip condition is taken as the condition. The microchannel geometry involved in this study are rectangular and parallel plate. In this study, heat transfer through the microchannel, two phase flow and other channel geometry will not be covered. The heat transfer issue is always investigated along with the fluid flow in microchannel in most of the study. Therefore, this study has the limitation in terms of heat transfer aspects and it is not suitable to be the reference for two phase flow in microchannel and of other geometry except for rectangular and parallel plate. Besides that, the fluid flow will be assumed as adiabatic flow and only hydrodynamic entrance length will be focused and to be studied but not thermally entrance length.

## **CHAPTER TWO: LITERATURE REVIEW**

### 2.1 Research Background

From the existing research works done related to this topic, most of the research works done deal with the flow in microchannel and the effect of hydraulic diameter and aspect ratio on hydraulic entrance length. The study of flow in microchannel is mainly focused on the pressure drop, drag in microchannels at laminar, transient and turbulent single phase flows in microchannel of different geometry, determination of range of Reynold Number at transition from laminar to turbulent, heat transfer of liquid and gas flows in small channels, and two phase flow in adiabatic and heated microchannels. Then the experimental data will be compared with the conventional theory. For the later study, it is focused on computing the correlation between dimensionless entrance length  $L_e/D_h$  and Reynold Number with respect to a range of aspect ratio, Reynold Number and different geometry of microchannel.

The challenges of this study are no any available or approved theory regarding the fluid flow in microchannel as its flow is totally different from flow in macrochannel. For instance, based on the study out by Morini on the summarisation of experimental work in mini and micro channels ( $D_h < 1.0$  mm) carried out till 2004 [12], he discovered that in many cases the experimental data of Poiseuille Number,  $Po$  which is dimensionless parameter used in calculation of drag, does not comply with the conventional theory. In addition, the experimental result of each study is inconsistent with each other. The discrepancies between the experimental works may have been attributed to rarefaction, compressibility effects, viscous dissipation, electro osmotic effects, property variation effects, channel surface conditions due to relative roughness and morphology as well as experimental uncertainties. These few reasons are invoked to illustrate the abnormal behaviour of transport mechanisms in mini and micro channels. For range of the laminar, transition and turbulent flow in microchannel, there is also discrepancies between each study that has been discussed in section 1.4.

In addition, there is no any standardized procedure and investigating methodology to carry out the study of flow in microchannel as well as the standardized definition regarding size of microchannel to provide uniformity. For instance, the classification scheme of microchannel based on hydraulic diameter of microchannel proposed by Kandlikar and Grande [13] which is recommended for the study of fluid flow of single phase as well as two-phase in microchannel does not seemed to be adopted by other

researches. In addition, by referring to Appendix 1 [14], it can be observed that some of the researches include pressure losses in their works while other does not and the working fluid used in some of the study differs with each other. For some of the study on flow in microchannel carried out by previous researches like Li et al., [15] Wu and Cheng, Sharp and Adrian [16] , and Cui et al [17]., deionized fluid is used as working fluid to avoid formation of electric double layer in liquid flow. When a liquid containing even a small number of ions flows over solid surfaces with electrostatic charges on their surface, the electrostatic charge on non-conducting surfaces attracts counter ions which have significant effect on the drag of flow and pressure drop in the microchannel. However, the thickness of this layer is very small, on the order of a few nm and the effect is negligible for hydraulic diameter of microchannel greater than  $10\mu\text{m}$ . [18]

Besides that, there is a lot of studies as well regarding entrance length of rectangular microchannel in which the correlation between dimensionless entrance length and Reynold number are different from each other due to experimental condition which has been discussed in section 1.4. Since previous studies are carried out by changing the aspect ratio which will change the hydraulic diameter as well for the rectangular microchannel and therefore the effect of these two factors on entrance length are of interest. Thus, the present numerical study examined these factors and the effect of hydraulic diameter was investigated by keeping the channel aspect ratio constant while the effect of aspect ratio was investigated by keeping the hydraulic diameter constant.

## CHAPTER 3: RESEARCH METHODOLOGY

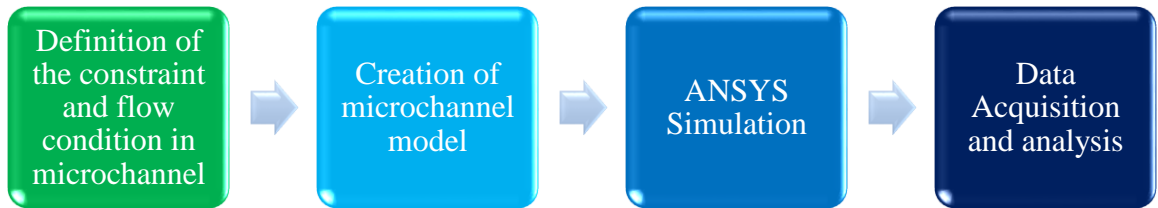


Figure 3.1: Flow Chart of Research Methodology

### 3.1 Constraint and Flow Condition in Microchannel

This study was carried out by using ANSYS FLUENT software to simulate the flow in rectangular microchannel with an aspect ratio and hydraulic diameter as well as flat plate or plane channel microchannel in order to gain the correlation between the dimensionless entrance length and Reynold number. Generally, the studies regarding flow in microchannel is based on the assumptions as shown below [19]. The assumptions include

- 1) The flow is created by a force due to a static pressure in the fluid.
- 2) The flow is stationary and fully developed which implies that it is strictly axial.
- 3) The flow regime in the microchannel is laminar flow.
- 4) There is no slip at the wall.
- 5) The fluids are incompressible Newtonian fluids with constant viscosity.
- 6) There is no heat transfer to or from the ambient medium.
- 7) The energy dissipation is negligible.
- 8) There is no fluid and wall interaction except for the fluid which is purely viscous.
- 9) The walls are straight.
- 10) The microchannel walls are smooth

Therefore, the above assumptions were the constraints and conditions of fluid flow in microchannel for this study. For microchannel with regular microstructure surface, assumption 10 is excluded.

### 3.2 Creation of Microchannel Model

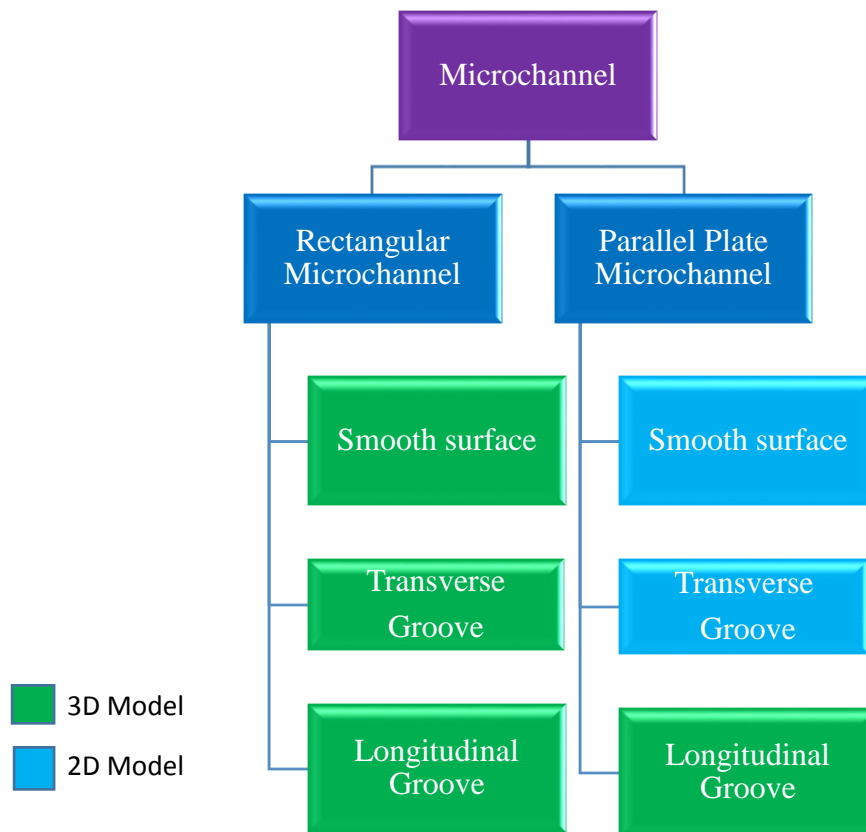


Figure 3.2: Schematic Diagram for Type of Regular Microstructure in Rectangular Microchannel and Parallel Plate Microchannel

Figure 3.2 showed the schematic diagram for the type of regular microstructure for both of the microchannel involved in this study. For both of the rectangular microchannel and parallel plate microchannel, there were three types of model created including the smooth surface, transverse groove and longitudinal groove. Microchannel model of smooth surface is the model that had no presence of microstructure on the surface of the microchannel model and its surface was smooth. For microchannel model with transverse and longitudinal groove, the microstructure are oriented transverse and parallel to the fluid flow in x direction respectively as shown in Figure 3.8. Among the types of regular microstructure for both types of microchannel, parallel plate microchannel of smooth surface and transverse groove were two dimensional (2D) model while the rest was three dimensional (3D) model. The reason of using 2D model instead 3D model for these two types of surface was due to its negligible effect from a third dimension as parallel plate microchannel model did not possess side walls which may impose an impact on fluid flow. In addition, the accuracy of result will be higher

and the duration of simulation will be shorter if 2D model is applied in this context. The dimension for parallel plate microchannel was 0.01m in length and 0.001m in height and its hydraulic diameter is equal to 2 times of height that is 0.002m. Rectangular microchannel had the same height and length as the parallel plate microchannel but with additional dimension of 0.001m in width which result in the aspect ratio of rectangular microchannel to be 1 and hydraulic diameter of 0.001m.

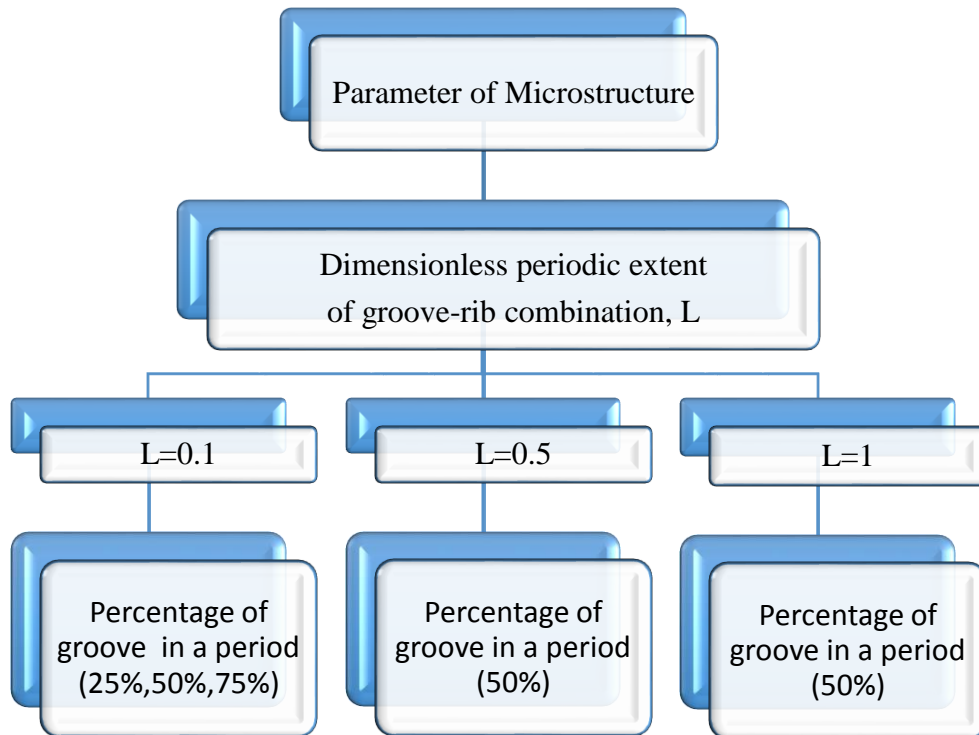


Figure 3.3: Schematic Diagram for Parameter and Sizing of Microstructure

Figure 3.3 depicted the parameter and sizing for the microstructure. The dimensionless period extent of groove-rib combination,  $L$  was the ratio of length for a period of combination of no slip wall (rib) with the shear free fraction (groove),  $E$  to the height of microchannel ( $H$ ) as shown in the equation below.

$$L = \frac{E}{H} \quad (6)$$

The length of a period would then be further subdivided into three category in which the portion or length for shear free fraction,  $e$  to occupy 25%, 50% and 75% of the length of a period,  $E$  for  $L=0.1$  only. For  $L=0.5$  and  $L=1.0$ , the length of a period,  $E$  will be divided into 50% shear free fraction. For instance, for 2D model of parallel plate microchannel with transverse groove surface and  $L=1$  with 75% of shear free fraction,

the length of a period,  $E$  was  $0.001\text{m}$  while the length of shear free fraction,  $e$  was  $0.00075\text{m}$ . The line highlighted with red color as shown in Figure 3.4 (iii) was the portion for shear free region. Similarly, for 3D model of rectangular microchannel with longitudinal groove surface and  $L=0.1$  with 25% of shear free fraction, the length of a period,  $E$  was  $0.0001\text{m}$  while the length of shear free fraction,  $e$  was  $0.000025\text{m}$ . The portion for shear free region of rectangular microchannel was as shown in Figure 3.4 (iv)

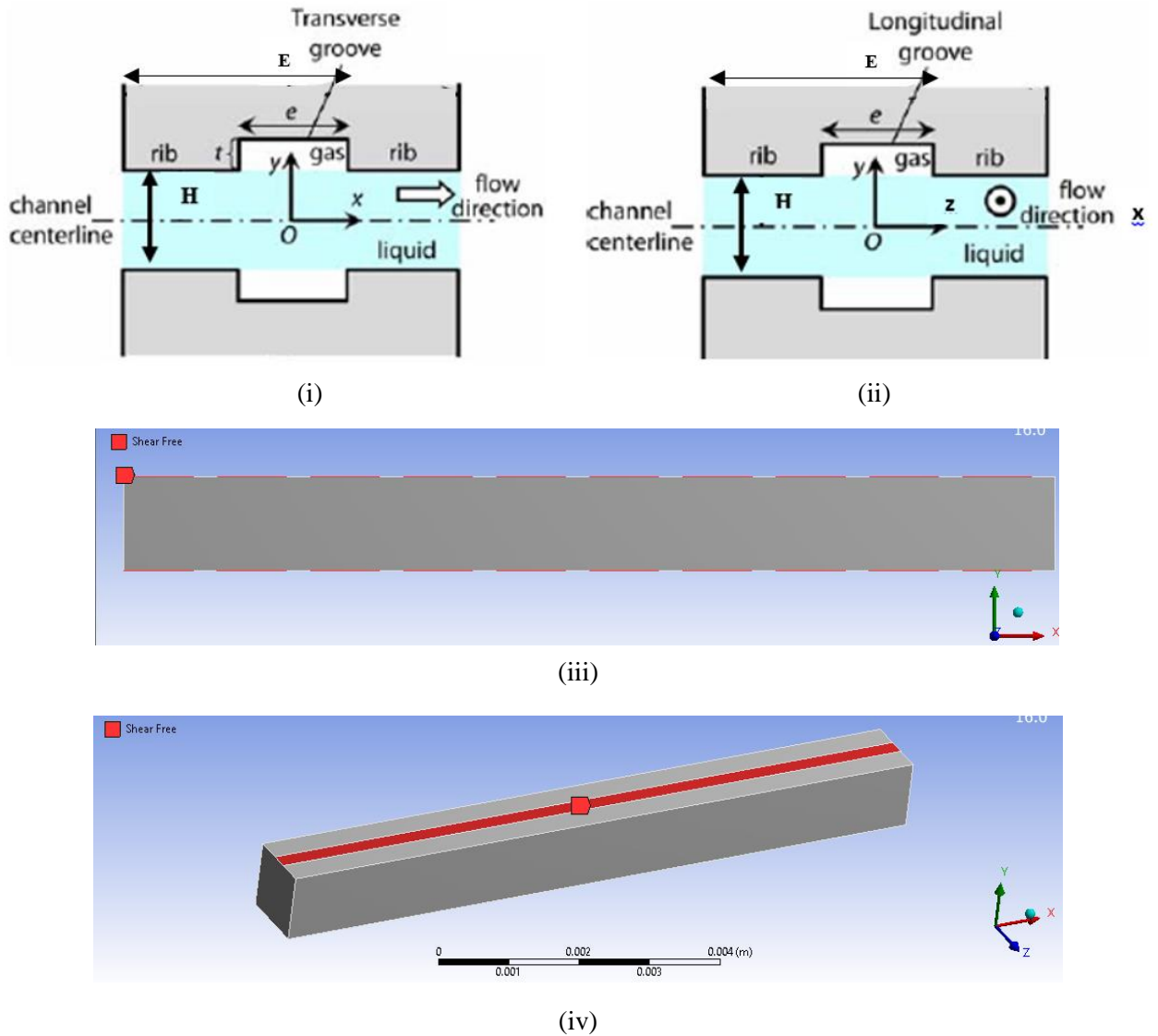

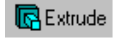




Figure 3.4: (i) and (ii) parameter of microstructure for both transverse and longitudinal groove, [20] (iii) Shear free region of 2D model parallel plate microchannel with transverse groove. (iv) Shear free region of 3D model rectangular microchannel with longitudinal groove.

Both the 2D and 3D model were created by using design modeler under fluid flow (fluent) toolbox in the ansys workbench. For 2D model of parallel plate microchannel with smooth surface, it is created by first sketching a rectangle of length of 0.01m and height of 0.001m followed by surface generation by using “Surface from Sketches” function (  ). For 3D model, the method was the same as the 2D model but with additional steps to create a 3D rectangular block that was by using “Extrude” function (  ) to create a rectangular block of 0.001m after the sketching of rectangular of size 0.01m in length and 0.001m in height on XY plane without generating surface for the sketch. For 3D model parallel plate microchannel with longitudinal groove, the dimension of the rectangular block was actually the size for a period of groove-rib combination but not the whole size of parallel plate microchannel. For instance, for  $L=0.1$  with 25% of shear free fraction, the size of the rectangular block would be 0.01m in length, 0.001m in height which was the same with other 2D and 3D model but with width of 0.0001m. Both of the two sides of upper and lower surface of the rectangular block would be 75% no slip surface with 25% of shear free fraction at the center. For 2D model and 3D model of transverse groove surface regardless type of microchannel, the surface condition in microchannel would be always started with no slip condition followed by shear free condition and repeated in an alternating manner. For 3D model of longitudinal groove surface regardless of the type of channel, both of the two side of upper and lower surface of the rectangular block would always be the no slip condition with repeating of shear free and no slip surface in alternating manner in between.

For 2D model of parallel plate microchannel with transverse groove surface, the method was basically the same as the smooth surface and additional steps were require to create the shear free fraction (groove) and no slip surface (rib). For no slip surface and shear free fraction, it was created by using “Split Edge” function (  ) and there were many ways to split the edge including split by N, split by delta, split by fractional and split by edge. To split an edge, the desired edge to be split had to be selected by using “Edge Selection Filter” (  ) followed by selection of appropriate splitting method. For 2D model, 2 edges were chosen while 4 edges were required to be split for 3D model. For 2D model and 3D model with transverse groove, the edges to be split were the edges along the x axis while the edges to be split for 3D model with longitudinal groove were the edges along the z-axis. The splitting methods involved in



the creation of 2D and 3D model for this study were “Split by N” and “Split by Delta”. For “Split by N” method, N represent the number of pieces to be split for an edge and the maximum number of pieces to be split is 100. The edges would be split into segments of equal length, except when the Sigma and Omega properties are defined. The Sigma property specifies the length of the first segment, while the Omega property defines the length of the last segment. The value of Sigma and Omega were both zero by default, which means all resultant segments will be of equal length. When the number of pieces to be split exceed 100, “Split by Delta” could be used instead of “Split by N”. For this method, the value for Delta specified the distance between each split along the edge. The length of the first segment however, was determined by the Sigma value. Splits were made until the remaining edge length was less than the Delta value. If the Sigma property is zero, then the length of the first segment will be equivalent to the Delta value. For instance, in order to create a 2D model of parallel plate microchannel with transverse groove surface and  $L=0.1$  and 25% shear free fraction, the length of a period, E was 0.0001m which implied there were 100 periods for microchannel length of 0.01m. The single period had to be further split into 4 equal parts which meant edge had to be split into 400 pieces. In this case, “Split by Delta” was used instead of “Split by N” to split the edge. Depending on the portion for shear free fraction, the number of pieces for a period to be chosen was different. For instance, for 25% shear free fraction, 1 out of 4 pieces of a period was chosen alternatively to be the shear free region which implied 100 pieces out of 400 pieces were shear free region along an edge. Figure 3.5 showed the difference between “Split by Delta” and “Split by N”.

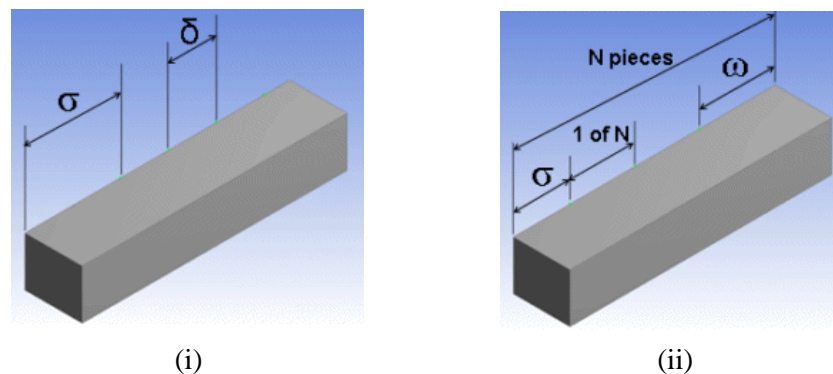
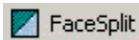

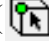
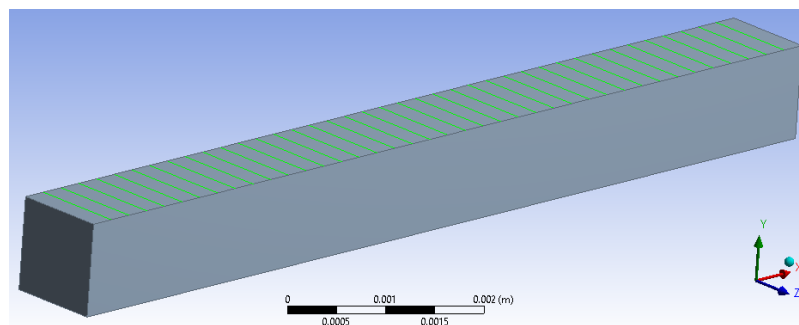


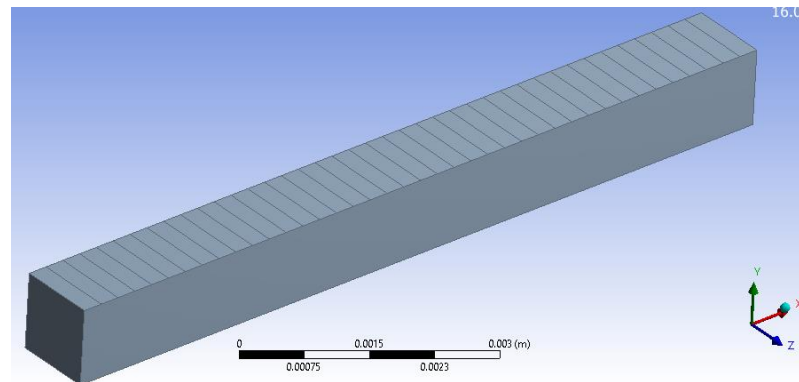
Figure 3.5: (i) Split by Delta, (ii) Split by N

For 3D model, the establishment for shear free region required additional steps to be completed. After splitting the necessary edges, “Face Split” (  ) was used to

split the desired surface into a number of surfaces depending on the number of pieces split along two parallel edges along x axis or z axis depending on the type of microstructure. The desired surface was selected by using “Face Selection Filter”. (  )The split surfaces was achieved by selecting the points created after edge splitting. The points can be selected by using “Points Selection Filter” (  ). The points chosen must be selected in the way that the two points must be opposite coherently with each other so that a perpendicular green straight line could be existed to connect the two points after selecting the two points as shown in Figure 3.6 (i). After finish selecting the points, the split surface can be generated and a resultant of split surfaces were created as shown in Figure 3.6 (ii).



(i)





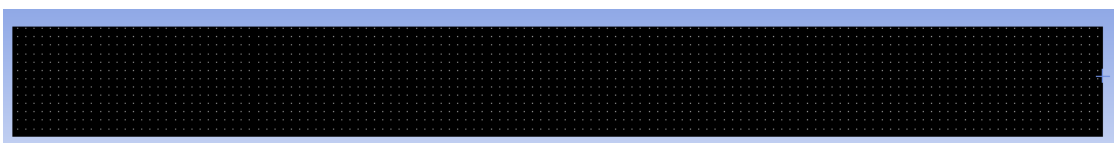
(b)

Figure 3.6: (i) Perpendicular green straight line joining the points along two parallel edges,  
(ii) Resultant Split surfaces

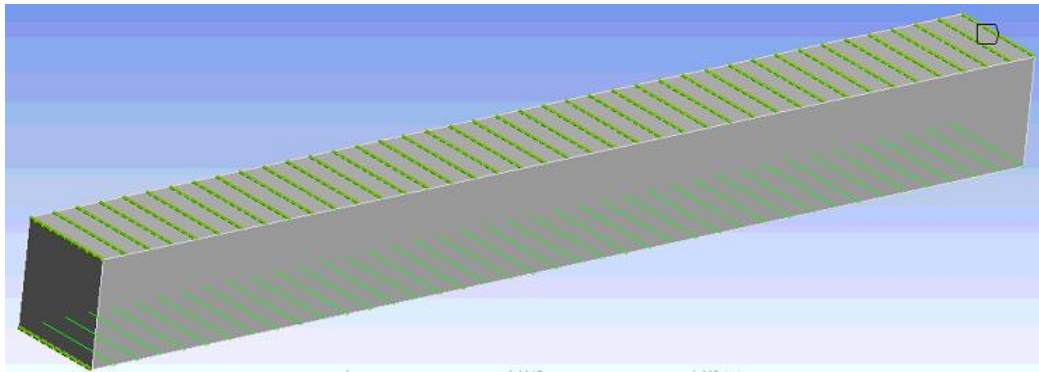
### 3.3 Ansys Simulation

The general steps to simulate developing flow in channel can be referred to the tutorial of developing flow in channel [21]. The simulation of the developing flow in channel only could be started after the completion of the model establishment on

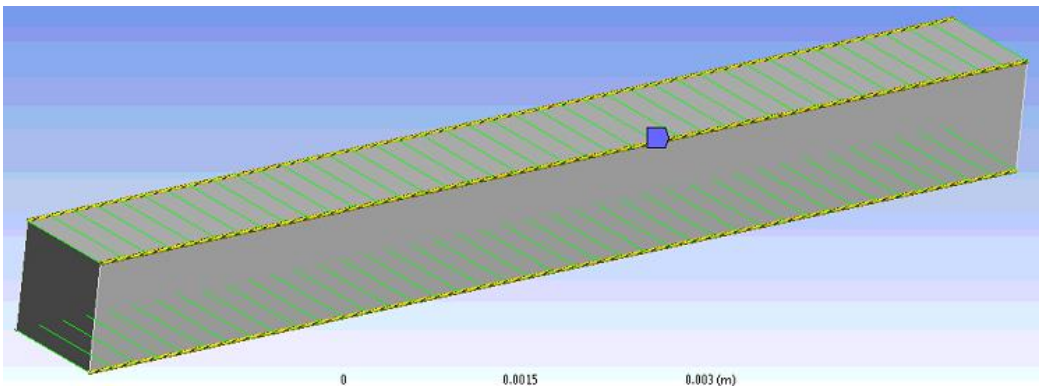
Geometry and Meshing Operation applied on the model on Mesh. In fact, the mesh element was generated manually by using “Face Meshing” (  Sizing ) and “ Sizing” (  Face Meshing ). Face meshing controls was used to generate a free or mapped mesh on selected faces. The Meshing application would determine an appropriate number of divisions for the edges on the boundary face automatically. If the number of divisions on the edge was specified with a “Sizing” control, the meshing application attempted to enforce those divisions on the selected surface. The surface meshing was done with quadrilateral method which implied the shape of the mesh element grid generated to be in quadrilateral shape. After applying “Face Meshing” on the desired surface, “Sizing” was applied and the desired edges were selected to manipulate the number of mesh element on a surface. For the behaviour of mesh element generated, it was set to “Hard” in order to get uniform and consistent mesh element in terms of shape and prevent the existence of irregular or deformed mesh element on the surface. For instance, to create a 64000 mesh or 800 mesh element along horizontal edge and 80 mesh element on the 2D parallel plate microchannel with transverse groove surface and  $L=1.0$  with 50% shear free fraction as shown in Figure 3.7 (i), the individual split edges for both upper and lower edge had to be divide into 40 division in order to achieve a 800 division along the upper and lower horizontal edge. For each of the upper and lower horizontal edge, it was split into 20 edges due to the parameter of microstructure whereby 2 edges represents a period. For the two vertical edges, it was selected and divide into 80 number division which was divided in the same way as the horizontal edges. For 3D model of transverse groove and longitudinal groove surface regardless type of microchannel, the relevant edges of microstructure should be selected in order to make sure the mesh element generated was consistent and constant in terms of shape. The number of the relevant edges were depending on the parameter of the microstructures. Figure 3.7 (ii), (iii),(iv) showed the relevant edges for the 3D model of transverse while the remaining were of longitudinal groove surface. Next, each of the part of the 2D and 3D model was defined as inlet, outlet, wall, shear free and symmetry as shown in Figure 3.8.



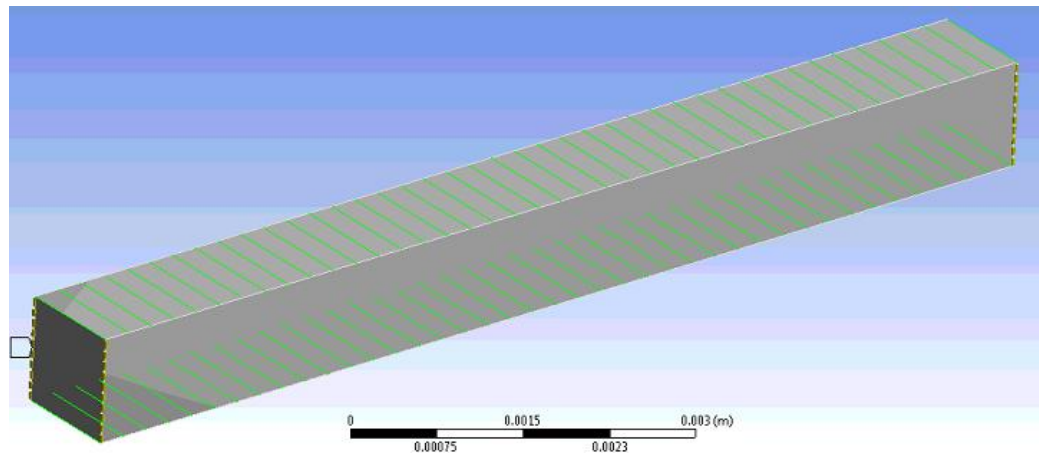
(i)



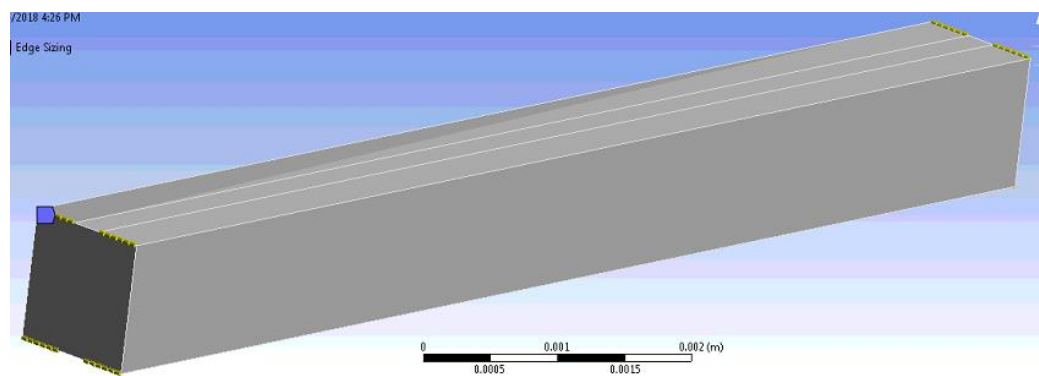
(ii)



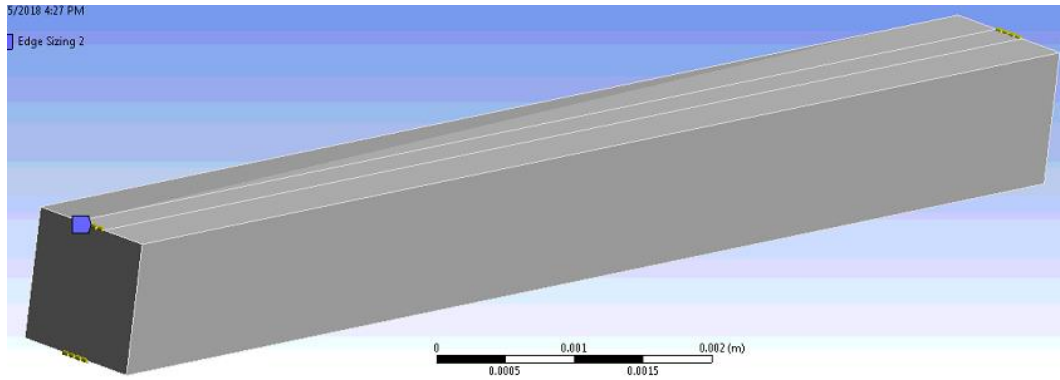
(iii)



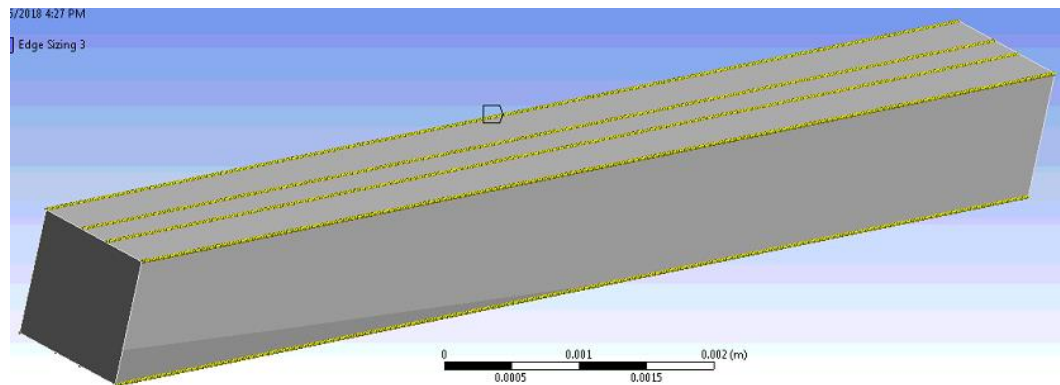
(iv)



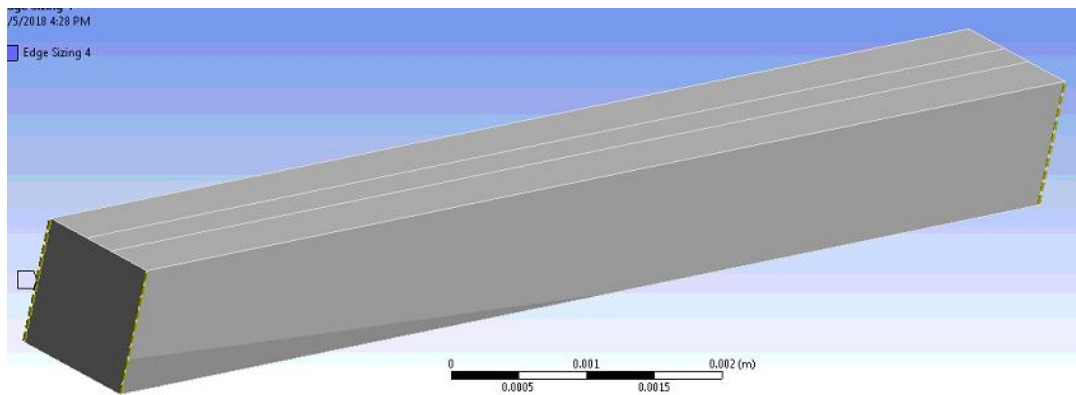
(v)



(vi)

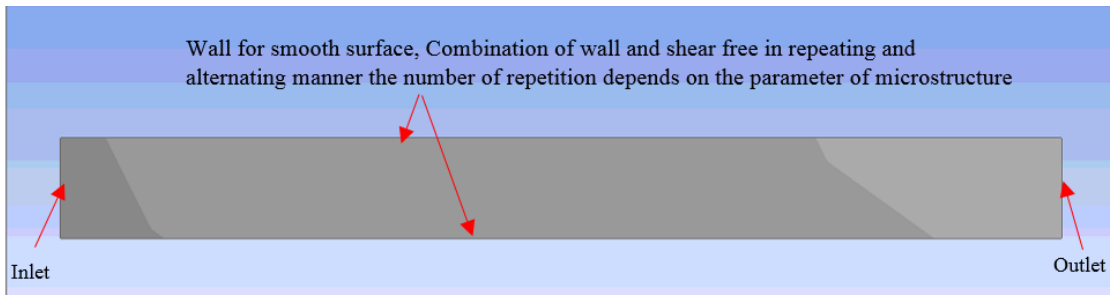


(vii)

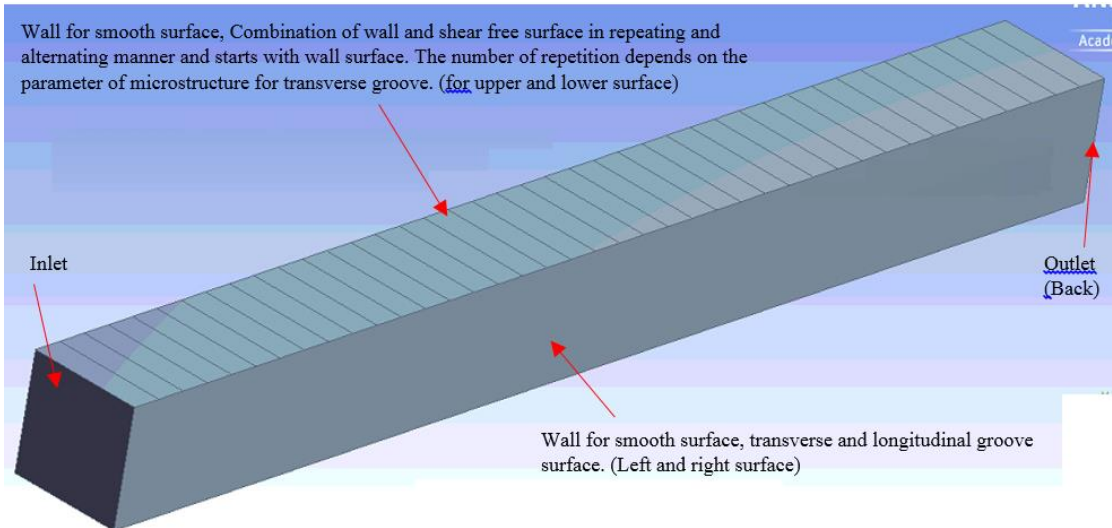


(viii)

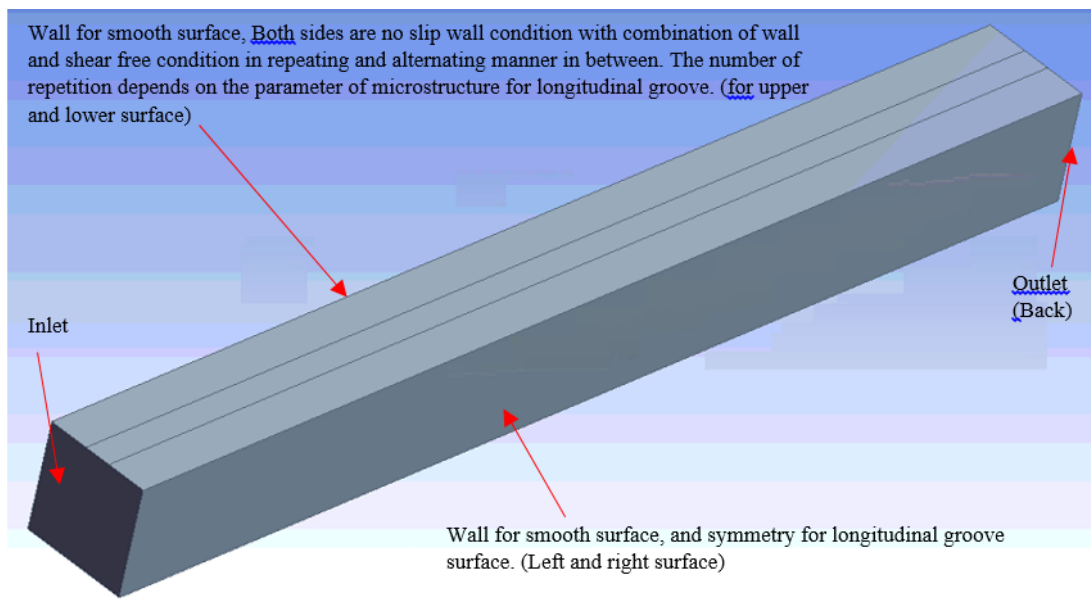
Figure 3.7: (i) Mesh element of 2D model, (ii, iii, iv) Relevant edges for meshing operation of 3D transverse groove model, (v, vi, vii, viii) Relevant edges for meshing operation of 3D longitudinal groove model



(i)



(ii)



(iii)

Figure 3.8: (i) Boundary Condition for 2D model of Parallel Plate Microchannel with Transverse Groove and Smooth Surface (ii) Boundary Condition for 3D model of Rectangular Microchannel with Transverse Groove (iii) Boundary Condition of 3D model of Rectangular and Parallel Plate Microchannel with Longitudinal Groove

### 3.3 Ansys Simulation

After finishing meshing operation, simulation could be started and the setting for simulation would be as mentioned in the tutorial of developing flow in channel [21] but with small change in configuration. The simulation setting for 2D model and 3D model basically were more or less the same. For the computing process, series processing was used for 2D simulation while parallel processing was used for 3D simulation to reduce the computation time. For both the simulation for 2D model and 3D model, the fluid used was water with density of  $1000 \text{ kg/m}^3$  and dynamic viscosity of  $0.001 \text{ kg/ms}$ . The setting of boundary condition for interior channel, outlet, and wall was the same as shown in Figure 3.8 for all 2D and 3D model. For 2D and 3D model with transverse or longitudinal groove surface, there would be an additional boundary which was the shear free fraction and “specified shear” was selected for shear condition. For setting of inlet, the value of velocity varies from  $0.000001 \text{ m/s}$ ,  $0.00001 \text{ m/s}$ ,  $0.0001 \text{ m/s}$  and  $0.001 \text{ m/s}$  for all 2D and 3D model depending on the Reynold Number of fluid flow simulated which ranged from 0.001, 0.01, 0.1 and 1 respectively. The simulation of all the 2D and 3D model would run on 1000 iterations without setting any convergence absolute criteria for x velocity, y velocity or z velocity. The convergence absolute criteria was the prescribed condition to end a simulation. For surface monitor, a center line was created by using “Line/ Rake” to monitor the convergence history of center x velocity. For 2D model, the values for the  $x_0$  and  $x_1$  were 0 and 0.01 respectively while the values of  $y_0$  and  $y_1$  were 0.0005. For 3D model, the values for  $x_0$ ,  $y_0$ ,  $x_1$  and  $y_1$  were the same as 2D model and with an additional values of 0.0005 for both  $z_0$  and  $z_1$ . The remaining setting for simulation such as model, solution method and solution control were the same as indicated in the tutorial of developing flow in channel [21]. After finishing configuring the setup for simulation, the simulation was initialised by using hybrid initialization followed by running the calculation with 1000 iterations.

### 3.4 Data Acquisition and Analysis

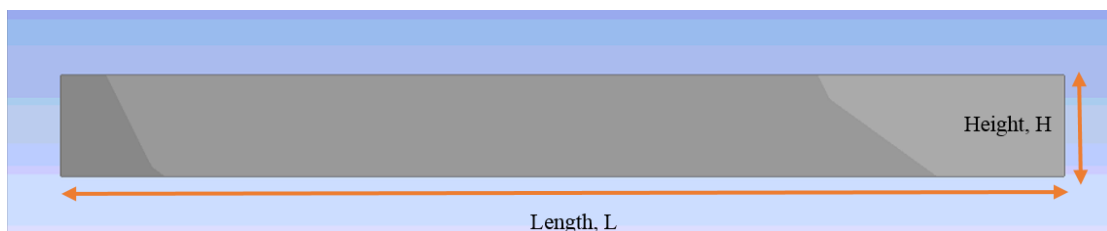
As this study was only focused on the hydrodynamic entrance length of the flow in microchannel, therefore the data of the center x velocity of the flow in the microchannel were of the interest. The steps to obtain the data for center x velocity could be referred to the tutorial of developing flow in channel at steps 29. After acquiring the necessary data, the data was exported as text file by clicking “Write to File” and it was processed by using MATLAB. Two MATLAB algorithms codes were written to process the data for center x velocity of fluid flow in microchannel with smooth surface and microchannel with transverse groove and longitudinal groove. Basically, the data of center x velocity for microchannel with smooth surface and microchannel with longitudinal groove were processed with the same algorithms while the other algorithms code was used to process the center x velocity of microchannel with transverse groove as shown in Appendix 3.



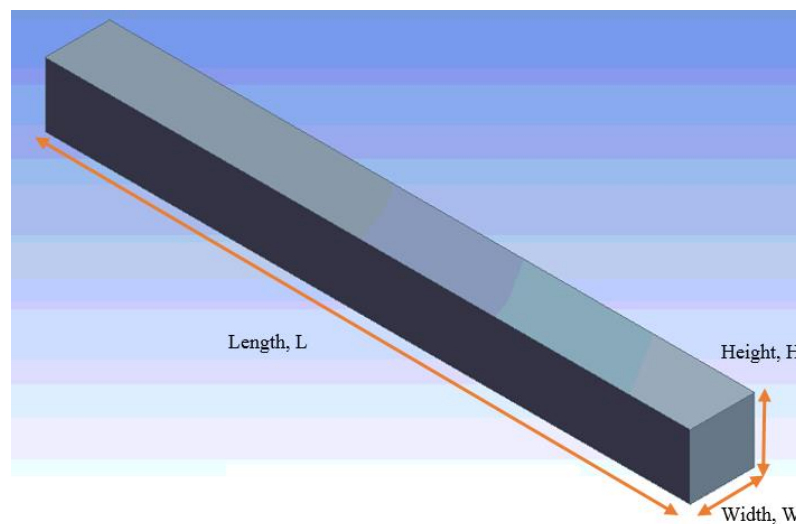
## CHAPTER 4: RESULT AND DISCUSSION

### 4.1 Results of Grid Independence Test

Figure 4.1 (i) and (ii) shows the dimension indication for 2D model which is for parallel plate microchannel and 3D model for rectangular microchannel as well as parallel plate microchannel of longitudinal groove. Before commencing simulation, the meshing of either 2D and 3D model is done and the resultant no of element of the model depends on the division separated on the length, height and width of the model. For instance, a 2D model of parallel plate microchannel with 4000 elements means there are 20 elements available on the height of the model while the length of the model are divided into 200 divisions. The number of element in the model will be listed out in the manner of [L x H] for 2D model and [L x W x H] for 3D model as shown in Table 4.1



(i)

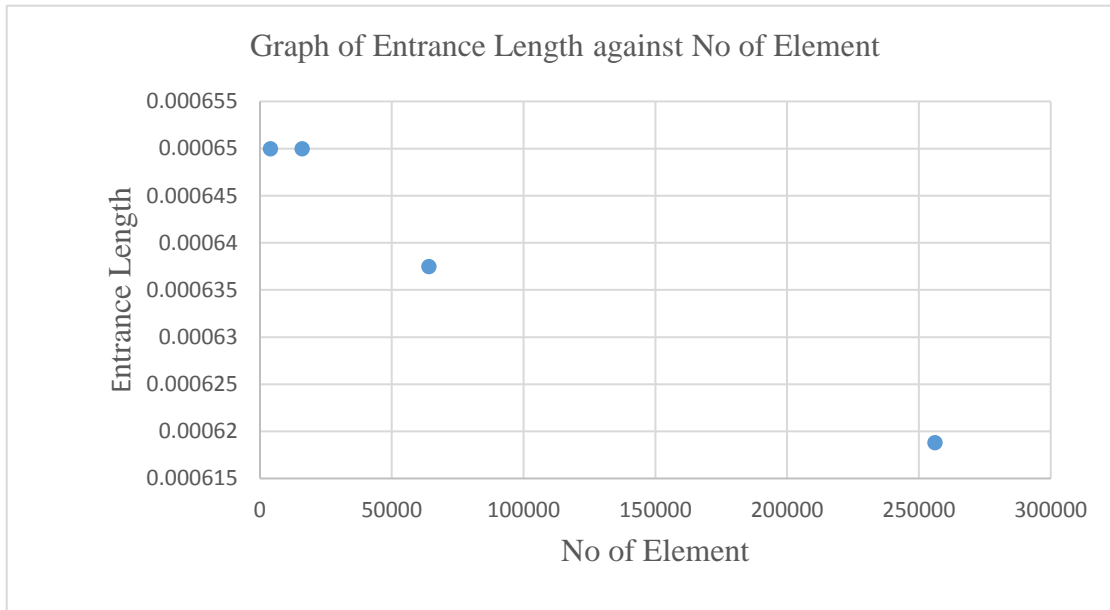


(ii)

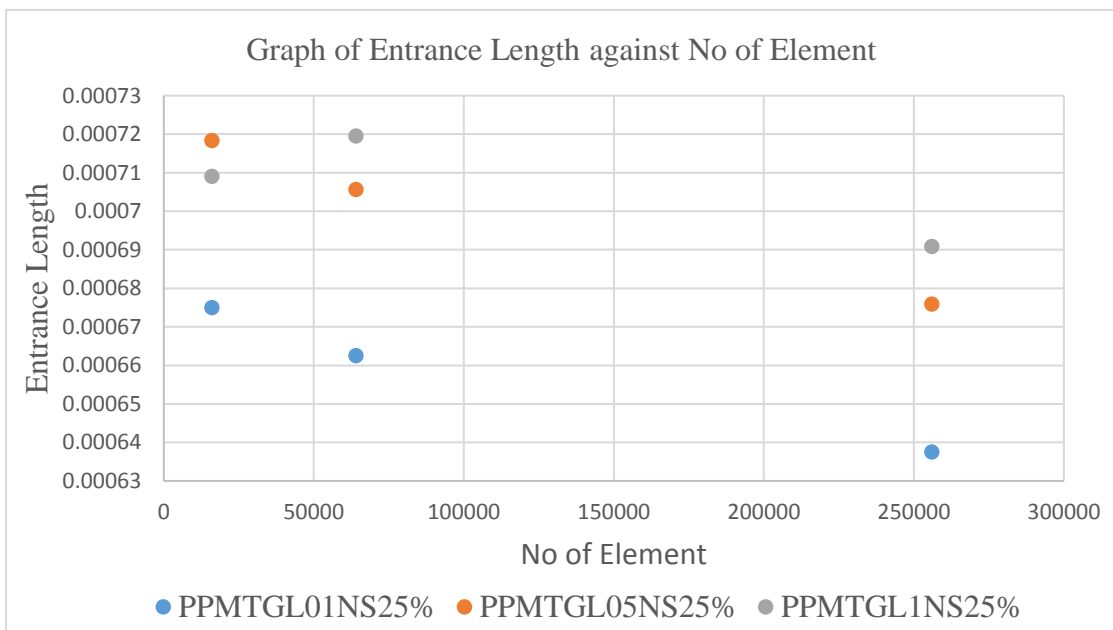
Figure 4.1: Dimension indication for (i) 2D model and (ii) 3D model

Grid Independence Test is carried out to determine the minimum number of element required for a simulation so as to optimize the computation time or the duration of simulation in order to acquire solution or result with higher accuracy. The grid independence test is carried out to determine the number of element required to simulate the fluid flow in 2D model of parallel plate microchannel with smooth surface and

transverse groove and 3D model of rectangular microchannel with smooth surface, transverse groove and longitudinal groove. Figure 4.2 and Figure 4.3 show the result for grid independence test for parallel plate microchannel and rectangular microchannel respectively. The results of grid independence test for parallel plate microchannel and rectangular microchannel are tabulated in Table 4.1 and Table 4.2 respectively. All the grid independence tests are carried out with Reynold Number of 0.001 corresponds to velocity of 0.000001 m/s.



(i)



(ii)